Measuring Dynamic *In-Vivo* Elbow Kinematics: Description of Technique and Estimation of Accuracy

Colin P. McDonald[1]
Bone and Joint Center,
Henry Ford Hospital,
2799 West Grand Boulevard,
Detroit, MI 48202
e-mail: colin.p.mcdonald@gmail.com

Vasilios Moutzouros
Department of Orthopaedics,
Henry Ford Hospital,
2799 West Grand Boulevard,
Detroit, MI 48202

Michael J. Bey
Bone and Joint Center,
Henry Ford Hospital,
2799 West Grand Boulevard,
Detroit, MI 48202

Background: The objectives of this study were to characterize the translational and rotational accuracy of a model-based tracking technique for quantifying elbow kinematics and to demonstrate its in vivo application. Method of Approach: The accuracy of a model-based tracking technique for quantifying elbow kinematics was determined in an in vitro experiment. Biplane X-ray images of a cadaveric elbow were acquired as it was manually moved through flexion-extension. The 3D position and orientation of each bone was determined using model-based tracking. For comparison, the position and orientation of each bone was also determined by tracking the position of implanted beads with dynamic radiostereometric analysis. Translations and rotations were calculated for both the ulnohumeral and radiohumeral joints, and compared between measurement techniques. To demonstrate the in vivo application of this technique, biplane X-ray images were acquired as a human subject extended their elbow from full flexion to full extension. Results: The in vitro validation demonstrated that the model-based tracking technique is capable of accurately measuring elbow motion, with reported errors averaging less than ±1.0 mm and ±1.0 deg. For the in vivo application, the carrying angle changed from an 8.3 ± 0.5 deg varus position in full flexion to an 8.4 ± 0.5 deg valgus position in full extension. Conclusions: Model-based tracking is an accurate technique for measuring in vivo, 3D, dynamic elbow motion. It is anticipated that this experimental approach will enhance our understanding of elbow motion under normal and pathologic conditions.
[DOI: 10.1115/1.4007951]

Keywords: elbow, motion analysis, validation, in vivo, accuracy

1 Introduction

The elbow is comprised of three bones, three joints and a group of several soft tissue structures. The elbow joint is classified as a trochleaginglymoid joint, producing both forearm rotation and flexion-extension; and its purpose is to position the hand in space. Significant research efforts have focused on studying the mechanics of the elbow. However, accurately quantifying elbow motion and joint interaction in 3D space, especially under *in vivo* conditions, remains a significant challenge.

Previous research on elbow kinematics has relied upon cadaveric simulations [1–12], *in vivo* motion capture or electromagnetic techniques [13–22], static radiography [23–25], and two-dimensional (2D) dynamic fluoroscopy [26] for quantifying the kinematics of the elbow. Cadaveric simulations are capable of providing highly accurate measures of joint position and motion. However, cadaveric simulations cannot completely reproduce the physical muscular force across the elbow. *In vivo* joint tracking techniques record kinematic data under a variety of dynamic conditions by tracking the position of skin mounted sensors or reflective markers. However, the externally positioned markers are susceptible to errors introduced by skin movement. Static radiography provides a noninvasive means to make accurate measurements at the elbow joint *in vivo*, and is often used to quantify the position and orientation of the elbow's flexion-extension axis [23–25]. However, this technique is limited to measurements at static positions of elbow flexion. Two-dimensional (2D) dynamic fluoroscopy can assess elbow translations and rotations throughout the full range of motion by registration of planar 2D fluoroscopic images to a three-dimensional (3D) imaging modality (such as computed tomography). However, these studies are restricted to quantifying single-plane measurements. For example, although sagittal images are ideal for measuring elbow range of motion, they cannot be used to measure the carrying angle of the ulna with respect to the humerus.

To overcome the limitations associated with previously reported techniques for measuring *in vivo* elbow kinematics, our laboratory has developed a method for tracking joint motion from biplane X-ray images based on their 3D shape and density [27]. This technique has been validated at other joints [27–31], but has not yet been applied to the elbow. The objectives of this study were to characterize the translational and rotational accuracy of this measurement technique and to demonstrate its *in vivo* application. Based on previous experience with this technique, we expected that the model-based tracking technique would be accurate to within approximately 1 mm in translation and 1 deg in rotation.

2 Materials and Methods

2.1 Validation of Model-Based Tracking Technique. Five 1.6 mm diameter tantalum beads were inserted into the distal humerus, proximal radius and proximal ulna of a human cadaveric specimen (right side). All soft tissues surrounding the elbow joint remained intact. The instruments for implanting the markers consisted of matched stainless steel cannulas, inserts, and drill guides with depth stops. The cannula/insert was used to drill a hole through the bone. The insert was removed and a bead was inserted into the cannula surrounded by bone wax and pushed to the end of the hole. The position of each bead within bone was verified using radiographic images. The specimen was secured to a custom apparatus with the elbow joint centered within the 3D imaging volume of a biplane X-ray system. Biplane X-ray images were acquired as the specimen was manually moved from a position of 135 deg flexion to full extension. This motion was performed three times. Biplane X-ray images were also acquired for three static trials, with the elbow fixed in full extension. The biplane X-ray images were acquired at 60 Hz for two seconds with the X-ray generators in pulsed mode (70 KV, 160 mA) and video cameras shuttered at 1/250 seconds to eliminate motion blur.

Following testing, CT images of the cadaveric arm, from mid-humerus to the wrist, were acquired using a clinical scanner (GE Medical Systems – LightSpeed VCT, New Berlin, WI, USA). Imaging parameters included a field of view of 128 mm, a

[1]Corresponding author.

Contributed by the Bioengineering Division of ASME for publication in the JOURNAL OF BIOMECHANICAL ENGINEERING. Manuscript received March 28, 2012; final manuscript received October 11, 2012; accepted manuscript posted October 25, 2012; published online November 27, 2012. Assoc. Editor: Richard E. Debski.

512×512 reconstruction matrix, and a voxel size of $0.25 \times 0.25 \times 0.60$ mm. The CT images of the humerus, radius and ulna were then segmented from surrounding bones and soft tissues using commercial software (Mimics 13.0, Materialise, Leuven, Belgium) and reconstructed to generate 3D bone models.

The 3D position and orientation of each bone was determined from the biplane X-ray images using a model-based tracking technique [27,30]. Briefly, this technique generates a pair of digitally reconstructed radiographs (DRRs) by ray-traced projection through the CT bone model. 3D position and orientation of a given bone can then be estimated by optimizing the correlation between the two DRRs and the two biplane X-ray images. This technique allowed for the independent determination of the 3D position and orientation of one bone relative to an adjacent bone for all frames of each trial. For comparison, the 3D position and orientation of each bone was also determined using the dynamic RSA technique and the implanted beads [32]. This represented the gold standard bone position, and was used to quantify the accuracy of the model-based tracking technique. This RSA technique has been shown to be accurate to within ± 0.1 mm [32].

In order to report the accuracy of the model-based tracking technique in clinically relevant terms, each bone's 3D position and orientation was first determined relative to a laboratory-based coordinate system for both the model-based tracking and dynamic RSA techniques. For each technique, we then transformed the data expressed in the laboratory-based coordinate system to the CT-based anatomical coordinate system. This anatomical coordinate system, determined from the CT bone model, was created for each bone using custom software [4,5,8]. For the humerus, three anatomic landmarks were selected: the center of the capitellum (defined as a sphere), the center of the trochlea (defined as a circle) and the center of the humeral medullary canal approximately 100 mm from the most distal point on the humerus. The local anatomic coordinate system was defined by three orthogonal vectors. The center of the capitellum and trochlea defined the flexion-extension axis, which was nominally aligned in the medial-lateral (ML) direction. The Z-axis (termed: PD-axis) was defined as the midpoint of the flexion-extension axis and the center of the medullary canal, and was oriented in the proximal-distal (PD) direction. The X-axis (termed: AP-axis) was defined as the vector cross-product of the PD-axis and the flexion-extension axis, and was oriented in the anterior-posterior (AP) direction. Lastly, the Y-axis (termed: ML-axis) was defined as the vector cross-product of the PD-axis and AP-axis, and was oriented in the medial-lateral direction [Fig. 1(*a*)].

For the radius, the three anatomic landmarks were the center of the radial head, the radial styloid, and the center of the medial distal radialulnar joint (DRUJ) surface. For the anatomic coordinate system, the PD-axis was defined as a vector starting at the medial DRUJ surface and ending at the radial head. The center of the medial DRUJ surface and radial styloid defined the distal-radial vector. The ML-axis was defined as the cross-product of the PD-axis and the distal-radial vector. Finally, the AP-axis was defined as the cross-product of the ML-axis and PD-axis [Fig. 1(*b*)].

For the ulna, the three anatomic landmarks were the center of the greater sigmoid notch, the proximal tip of the olecranon, and the distal ulnar styloid. The proximal tip of the olecranon and distal ulnar styloid defined the long-axis of the ulna, and was nominally aligned in the proximal-distal direction. The ML-axis was defined as the cross-product of the long-axis of the ulna and a vector defined by the center of the greater sigmoid notch and the proximal tip of the olecranon. The AP-axis was defined as the cross-product of the ML-axis and the long-axis of the ulna. Finally, the PD-axis was defined as the cross-product of the AP-axis and ML-axis [Fig. 1(*c*)].

For each elbow extension trial, 3D kinematics (i.e., translations and rotations) of the elbow were calculated based on the position and orientation data determined from the biplane X-ray images using an Eulerian angle analysis. An Euler angle sequence of flexion-extension, varus-valgus rotation, and internal-external rotation was selected based on previous reports of elbow kinematic analysis [8,11,33,34]. Translations and rotations were calculated for both the ulnohumeral and radiohumeral joints. Flexion-extension was defined as rotation about the ML-axis of the humerus, varus-valgus rotation was defined as rotation about the AP-axis of the humerus, and internal-external rotation was defined as rotation about the PD-axis of the humerus. AP translation was defined as translation along the AP-axis, ML translation was defined as translation long the ML-axis, and PD translation was defined as translation along the PD-axis. Expressing these kinematic data in a common anatomical coordinate system allowed for a direct comparison between the model-based tracking and dynamic RSA techniques.

Translational and rotational accuracy were quantified in terms of bias, precision, and dynamic accuracy [35]. Bias was defined as the mean difference between the two measurement techniques (model-based tracking and dynamic RSA) during the dynamic trials. Precision was defined as the standard deviation of the model-based measurements when applied to only the static trials (30 frames per static trial). Thus, any frame-to-frame variability in measurement error when no motion occurred provided an estimate of the precision of the model-based tracking technique. To provide a single measure of accuracy, dynamic accuracy was defined as the root mean square error between the two measurement techniques during the dynamic trials. Bias and dynamic accuracy were

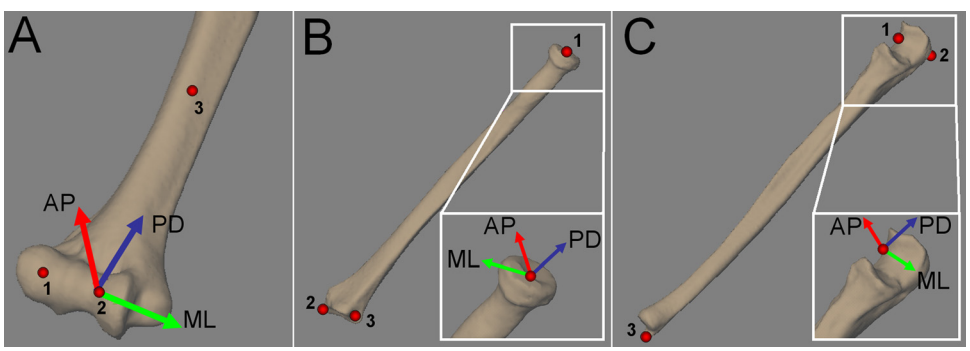

Fig. 1 Anatomical coordinate systems were created for the humerus (*a*), radius (*b*), and ulna (*c*). For the humerus, anatomic landmarks included the capitellum [panel (*a*);1], trochlea [panel (*b*);2], and center of the medullary canal [panel (*a*);3]. For the radius, anatomic landmarks included the center of the radial head [panel (*b*);1], the radial styloid [panel (*b*);2], and the center of the medial distal radialulnar joint surface [panel (*b*);3]. For the ulna, anatomic landmarks included the center of the greater sigmoid notch [panel (*c*);1], the proximal tip of the olecranon [panel (*c*);2], and the distal ulnar styloid [panel (*c*);3].

calculated for each frame in the three dynamic trials, and reported as the mean ± one standard deviation of all 360 frames (three trials at 120 frames per trial). Precision was calculated for each static trial, and reported as the mean ± one standard deviation of the three trials. Bias, precision and dynamic accuracy were calculated for each kinematic outcome measure (three translations and three rotations) of each joint. A *t* test was used to determine if the bias was significantly different than zero, with significance set at $p < 0.05$.

2.2 *In-Vivo* Application. To demonstrate *in vivo* application of the model-based tracking technique, one subject (male, age 27) with no history of previous elbow injury or surgery was tested. Following IRB approval and informed consent, the subject was seated with their right shoulder externally rotated and abducted 90 deg, and their right elbow resting on a platform and centered in the biplane X-ray system. With the forearm in full supination, biplane X-ray images were acquired at 60 Hz while the subject extended their right elbow from full flexion to full extension. Three dynamic trials were collected.

Following biplane X-ray testing, a CT image of the subject's right arm, from mid-humerus to the wrist, was acquired. Imaging parameters included a field of view of 180 mm, a 512×512 reconstruction matrix, and a voxel size of $0.35 \times 0.35 \times 0.60$ mm. Individual 3D bone models of the humerus, radius, and ulna were created by manually segmenting each bone from other surrounding bones and soft tissues using commercial software (Mimics 13.0, Materialise, Leuven, Belgium).

The 3D position and orientation of each bone was determined using the model-based tracking technique [27]. An anatomic coordinate system was created for the humerus, radius, and ulna using anatomic landmarks and vector cross-products [4,5,8]. 3D kinematics of the elbow were calculated based on the position and orientation data determined from the biplane X-ray images [8,11,33,34]. Kinematic outcome measures were averaged across the three motion trials, and included flexion-extension range of motion and the carrying angle. The carrying angle throughout elbow flexion was calculated as the varus-valgus angle of the ulna with respect to the humerus.

3 Results

3.1 Validation of Model-Based Tracking Technique. The model-based tracking technique produced results that were in close agreement with the RSA technique. At the ulnohumeral joint (Table 1), average translational bias ranged from −0.26 to 0.35 mm and was not significantly different than zero ($p = 0.13$). Average rotational bias ranged from −0.75 deg to −0.03 deg and was found to be significantly different than zero ($p < 0.05$). Average precision was less than 0.20 mm and 0.42 deg. Average dynamic accuracy was within 0.72 mm and 0.91 deg.

At the radiohumeral joint (Table 2), average translational bias ranged from −0.60 to 0.48 mm and was found to be significantly different than zero ($p < 0.05$). Average rotational bias ranged from −0.51 deg to −0.36 deg and was not significantly different than zero ($p = 0.11$). Average precision was less than 0.41 mm and 0.30 deg. Average dynamic accuracy was within 0.96 mm and 0.97 deg.

3.2 *In-Vivo* Application. For the representative subject, mean elbow extension was 0.9 ± 0.5 deg, mean elbow flexion was 144.5 ± 1.2 deg, and the average range of motion across the three motion trials was 143.7 ± 1.7 deg. The pattern of change in the carrying angles with elbow extension was consistent across the three motion trials (Fig. 2). As the elbow was extended, the carrying angle changed linearly from an 8.3 ± 0.5 deg varus position in full flexion to an 8.4 ± 0.5 deg valgus position in full extension.

4 Discussion

The objectives of this study were to characterize the translational and rotational accuracy of a model-based tracking technique for quantifying elbow kinematics, and to demonstrate its *in vivo* application. Using a well-validated and well-accepted dynamic RSA technique as a gold standard [32], this study demonstrated that the model-based tracking technique is capable of accurately measuring elbow motion, with reported errors averaging less than ±1.0 mm in translation and ±1.0 deg in rotation. In addition, the study demonstrated *in vivo* application of the measurement technique and reported the results from one subject that was in agreement with previous literature [11,33,36–39].

The model-based tracking technique produced results that were, in general, in close agreement with the RSA technique. However, there were larger errors between the two techniques in some frames, with dynamic accuracy ranging from 0.1 to 1.7 mm and from 0.1 to 1.8 deg across all frames of the dynamic trials. These higher errors in dynamic accuracy may have been due to the relative position of the radius and ulna within the biplane X-ray system. For portions of flexion-extension, the radial head and ulnar shaft overlapped one another, possibly affecting alignment using the model-based tracking technique. The exact frames of overlap varied from trial-to-trial, but were generally during mid-flexion. This may explain why the measurement bias between the model-based tracking technique and dynamic RSA technique was, in some instances, significantly different than zero. It may also explain why the model-based tracking technique, when applied to the elbow, was found to be less accurate than previous studies conducted in our laboratory on other joints [27–30]. Adjusting forearm rotation as well as arm position within the X-ray field of view may reduce the degree of radial-ulnar overlap within the X-ray images, and subsequently improve the accuracy of the model-based tracking technique. However, this requires further investigation.

Elbow range of motion has been previously reported to range from 135–147 deg [38], whereas the carrying angle has been previously reported to range from 7–19 deg valgus in full extension and change linearly from valgus to varus as the elbow is flexed to

Table 1 Translational and rotational accuracy at the Ulnohumeral Joint (characterized in terms of bias, precision, and dynamic accuracy). Translations are expressed in mm, rotations are expressed in degrees. Anterior-Posterior (AP), Medial-Lateral (ML), Proximal-Distal (PD), Flexion-Extension (FE), Varus-Valgus (VV), and IE – Internal-External (IE).

		Bias	Precision	Dynamic Accuracy
Translation (mm)	AP	−0.26 ± 0.73	0.10 ± 0.02	0.72 ± 0.23
	ML	0.35 ± 0.50	0.20 ± 0.07	0.49 ± 0.37
	PD	−0.15 ± 0.77	0.12 ± 0.01	0.70 ± 0.39
Rotation (degrees)	FE	−0.75 ± 0.59	0.08 ± 0.03	0.78 ± 0.62
	VV	−0.03 ± 1.27	0.14 ± 0.07	0.91 ± 0.52
	IE	−0.39 ± 0.64	0.42 ± 0.14	0.62 ± 0.43

Table 2 Translational and rotational accuracy at the Radiohumeral Joint (characterized in terms of bias, precision, and dynamic accuracy). Translations are expressed in mm, rotations are expressed in degrees. Anterior-Posterior (AP), Medial-Lateral (ML), Proximal-Distal (PD), Flexion-Extension (FE), Varus-Valgus (VV), and Internal-External (IE)

		Bias	Precision	Dynamic Accuracy
Translation (mm)	AP	−0.60 ± 0.61	0.33 ± 0.02	0.78 ± 0.47
	ML	0.46 ± 1.06	0.18 ± 0.07	0.96 ± 0.48
	PD	−0.48 ± 0.64	0.41 ± 0.02	0.70 ± 0.37
Rotation (degrees)	FE	−0.51 ± 0.75	0.17 ± 0.15	0.65 ± 0.71
	VV	−0.39 ± 1.17	0.21 ± 0.19	0.97 ± 0.62
	IE	−0.36 ± 0.86	0.30 ± 0.18	0.72 ± 0.68

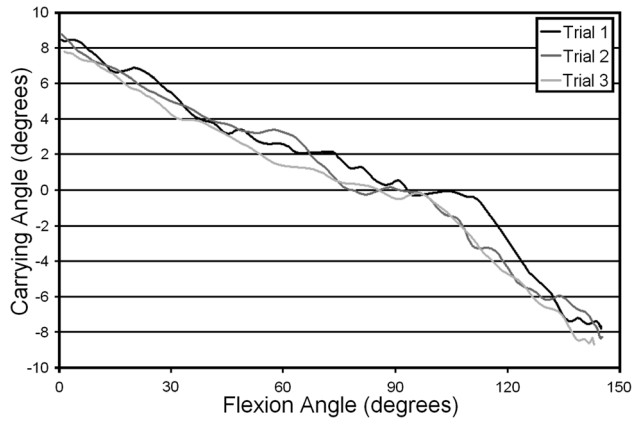

Fig. 2 The change in the average carrying angle with elbow flexion angle for the ulnohumeral joint is shown for one representative subject across three motion trials. A 0° flexion angle represents full extension. For the carrying angle, valgus angulation is positive, and varus angulation is negative.

full flexion [40–42]. In this investigation, the path of motion for one representative subject was consistent across three motion trials, and the subject exhibited motion characteristics that were consistent with what has been previously reported in the literature [11,33,36–39].

Accurately measuring *in vivo* elbow kinematics is important for understanding, among other things, the etiology of ligament injuries and the effects of surgical treatment to correct these injuries. Unfortunately, there are few studies investigating *in vivo* elbow kinematics, and the accuracy of the techniques employed in these studies is rarely reported. In the investigation of elbow kinematics, a technique that is accurate to within ±1.0 mm and ±1.0 deg is necessary to detect subtle changes in joint position that may occur with injury. For example, injury to the ulnar collateral ligament mechanically alters elbow function, increasing medial joint spacing and varus-valgus laxity, and resulting in joint instability. Medial joint spacing (based on interbone distance measurements) and varus-laxity laxity has been reported to be approximately 3–4 mm and 6–9 deg, respectively, in the normal elbow joint, whereas deficiency of the ulnar collateral ligament has been reported to increase medial joint spacing and varus-valgus laxity by 2–4 mm and 4–10 deg, respectively [43,44]. The technique reported here is capable of detecting changes in joint position within these levels.

The strength of the experimental approach described here is that it provides accurate noninvasive measures of *in vivo* elbow motion during dynamic activities. Limitations include radiation safety concerns that restrict the number of trials that can be acquired for a given subject, and the size of the biplane X-ray system's 3D field of view which limits the activities during which elbow motion can be measured. The use of one specimen is another limitation of this study, as a single specimen does not account for variations in bony anatomy, soft tissue structure, bone density, and other factors that affect image quality. However, this specific model-based tracking technique has been evaluated for a wide variety of joints with gross differences in bony anatomy, soft tissue structure, and bone density. Despite gross differences in imaging conditions and image quality between these anatomical joints, these previous validation studies have consistently reported translational and rotational errors ranging from approximately 0.4 to 0.7 mm and 0.5 to 0.9 degrees [27–31]. The consistency of these previously reported findings strongly suggests that variations in imaging conditions within the *same* joint due to subtle differences in anatomy, soft-tissue, or bone density are likely to have a relatively minor effect on accuracy of the model-based tracking technique. Consequently, it is unlikely that testing additional elbow specimens would have an appreciable effect on the accuracy values presented here. This study further supports the use of model-based tracking as an accurate technique for the measure of joint motion, and applies it specifically towards the elbow joint.

This study examined the accuracy of a model-based tracking technique for measuring elbow kinematics. The results of this study demonstrate that this method is capable of accurately measuring elbow motion, with errors averaging less than ±1.0 mm in translation and ±1.0 deg in rotation. This noninvasive technique has several applications in the study of elbow kinematics. Future efforts will focus on applying this technique towards the study of interactions at the joint, which is important in the study of postoperative mechanics following surgical treatment for elbow disorders such as ligament reconstructions and total elbow arthroplasty.

Conflict of Interest Statement

The authors, their immediate families, and any research foundations with which they are affiliated did not receive any financial payments or other benefits from any entity related to the subject of this article.

Acknowledgment

The authors wish to acknowledge the funding provided by the department of orthopaedic surgery at Henry Ford Hospital.

References

[1] An, K. N., 2005, "Kinematics and Constraint of Total Elbow Arthroplasty," J. Shoulder Elbow Surg., **14**(1S), pp. 168S–173S.
[2] Bottlang, M., Madey, S. M., Steyers, C. M., Marsh, J. L., and Brown, T. D., 2000, "Assessment of Elbow Joint Kinematics in Passive Motion by Electromagnetic Motion Tracking," J. Orthop. Res., **18**(2), pp. 195–202.
[3] Bottlang, M., O'Rourke, M. R., Madey, S. M., Steyers, C. M., Marsh, J. L., and Brown, T. D., 2000, "Radiographic Determinants of the Elbow Rotation Axis: Experimental Identification and Quantitative Validation," J. Orthop. Res., **18**(5), pp. 821–828.
[4] Duck, T. R., Dunning, C. E., Armstrong, A. D., Johnson, J. A., and King, G. J., 2003, "Application of Screw Displacement Axes to Quantify Elbow Instability," Clin. Biomech. (Bristol, Avon), **18**(4), pp. 303–310.
[5] Duck, T. R., Dunning, C. E., King, G. J., and Johnson, J. A., 2003, "Variability and Repeatability of the Flexion Axis at the Ulnohumeral Joint," J. Orthop. Res., **21**(3), pp. 399–404.
[6] Eygendaal, D., Olsen, B. S., Jensen, S. L., Seki, A., and Sojbjerg, J. O., 1999, "Kinematics of Partial and Total Ruptures of the Medial Collateral Ligament of the Elbow," J. Shoulder Elbow Surg., **8**(6), pp. 612–616.
[7] Floris, S., Olsen, B. S., Dalstra, M., Sojbjerg, J. O., and Sneppen, O., 1998, "The Medial Collateral Ligament of the Elbow Joint: Anatomy and Kinematics," J. Shoulder Elbow Surg., **77**(4), pp. 345–351.
[8] Johnson, J. A., Rath, D. A., Dunning, C. E., Roth, S. E., and King, G. J., 2000, "Simulation of Elbow and Forearm Motion *In Vitro* Using a Load Controlled Testing Apparatus," J. Biomech., **33**(5), pp. 635–639.
[9] Kamineni, S., Hirahara, H., Neale, P., O'Driscoll, S. W., An, K. N., and Morrey, B. F., 2007, "Effectiveness of the Lateral Unilateral Dynamic External Fixator After Elbow Ligament Injury," J. Bone Joint Surg. Am., **89**(8), pp. 1802–1809.
[10] King, G. J., Itoi, E., Niebur, G. L., Morrey, B. F., and An, K. N., 1994, "Motion and Laxity of the Capitellocondylar Total Elbow Prosthesis," J. Bone Joint Surg. Am., **76**(7), pp. 1000–1008.
[11] Morrey, B. F., and Chao, E. Y., 1976, "Passive Motion of the Elbow Joint," J. Bone Joint Surg. Am., **58**(4), pp. 501–508.
[12] Morrey, B. F., Tanaka, S., and An, K. N., 1991, "Valgus Stability of the Elbow. A Definition of Primary and Secondary Constraints," Clin. Orthop. Relat. Res. **265**, pp. 187–195.
[13] Cutti, A. G., Cappello, A., and Davalli, A., 2006, "*In Vivo* Validation of a New Technique that Compensates for Soft Tissue Artefact in the Upper-Arm: Preliminary Results," Clin. Biomech. (Bristol, Avon) **21**(1), pp. S13–S19.
[14] Fleisig, G. S., Bolt, B., Fortenbaugh, D., Wilk, K. E., and Andrews, J. R., 2011, "Biomechanical Comparison of Baseball Pitching and Long-Toss: Implications for Training and Rehabilitation," J. Orthop. Sports Phys. Ther., **41**(5), pp. 296–303.
[15] Huang, Y. H., Wu, T. Y., Learman, K. E., and Tsai, Y. S., 2010, "A Comparison of Throwing Kinematics Between Youth Baseball Players With and Without a History of Medial Elbow Pain," Chin. J. Physiol., **53**(3), pp. 160–166.
[16] Melchiorri, G., Padua, E., Padulo, J., D'Ottavio, S., Campagna, S., and Bonifazi, M., 2011, "Throwing Velocity and Kinematics in Elite Male Water Polo Players," J. Sports Med. Phys. Fitness, **51**(4), pp. 541–546.
[17] Nissen, C. W., Westwell, M., Ounpuu, S., Patel, M., Solomito, M., and Tate, J., 2009, "A Biomechanical Comparison of the Fastball and Curveball in Adolescent Baseball Pitchers," Am. J. Sports Med., **37**(8), pp. 1492–1498.

[18] Stokdijk, M., Biegstraaten, M., Ormel, W., de Boer, Y. A., Veeger, H. E., and Rozing, P. M., 2000, "Determining the Optimal Flexion-Extension Axis of the Elbow *In Vivo* – A Study of Interobserver and Intraobserver Reliability," J. Biomech., **33**(9), pp. 1139–1145.
[19] Stokdijk, M., Meskers, C. G., Veeger, H. E., de Boer, Y. A., and Rozing, P. M., 1999, "Determination of the Optimal Elbow Axis for Evaluation of Placement of Prostheses," Clin. Biomech. (Bristol, Avon) **14**(3), pp. 177–184.
[20] Werner, S. L., Guido, J. A., Delude, N. A., Stewart, G. W., Greenfield, J. H., and Meister, K., 2010, "Throwing Arm Dominance in Collegiate Baseball Pitching: A Biomechanical Study," Am. J. Sports Med., **38**(8), pp. 1606–1610.
[21] Werner, S. L., Guido, J. A., Jr., Stewart, G. W., McNeice, R. P., VanDyke, T., and Jones, D. G., 2007, "Relationships Between Throwing Mechanics and Shoulder Distraction in Collegiate Baseball Pitchers," J. Shoulder Elbow Surg., **16**(1), pp. 37–42.
[22] Chin, A., Lloyd, D., Alderson, J., Elliott, B., and Mills, P., 2010, "A Marker-Based Mean Finite Helical Axis Model to Determine Elbow Rotation Axes and Kinematics *In Vivo*," J. Appl. Biomech., **26**(3), pp. 305–315.
[23] Ericson, A., Arndt, A., Stark, A., Wretenberg, P., and Lundberg, A., 2003, "Variation in the Position and Orientation of the Elbow Flexion Axis," J. Bone Joint Surg. Br., **85**(4), pp. 538–544.
[24] Ericson, A., Stark, A., and Arndt, A., 2008, "Variation in the Position of the Elbow Flexion Axis After Total Joint Replacement With Three Different Prostheses," J. Shoulder Elbow Surg., **17**(5), pp. 760–767.
[25] London, J.T., 1981, "Kinematics of the Elbow," J. Bone Joint Surg. Am., **63**(4), pp. 529–535.
[26] Futai, K., Tomita, T., Yamazaki, T., Murase, T., Yoshikawa, H., and Sugamoto, K., 2010, "*In Vivo* Three-Dimensional Kinematics of Total Elbow Arthroplasty Using Fluoroscopic Imaging," Int. Orthop., **34**(6), pp. 847–854.
[27] Bey, M. J., Zauel, R., Brock, S. K., and Tashman, S., 2006, "Validation of a New Model-Based Tracking Technique for Measuring Three-Dimensional, *In Vivo* Glenohumeral Joint Kinematics," J. Biomech. Eng., **128**(4), pp. 604–609.
[28] Anderst, W., Zauel, R., Bishop, J., Demps, E., and Tashman, S., 2009, "Validation of Three-Dimensional Model-Based Tibio-Femoral Tracking During Running," Med. Eng. Phys., **31**(1), pp. 10–16.
[29] Bey, M. J., Kline, S. K., Tashman, S., and Zauel, R., 2008, "Accuracy of Biplane X-Ray Imaging Combined With Model-Based Tracking for Measuring *In Vivo* Patellofemoral Joint Motion," J. Orthop. Surg. Res., **3**, p. 38.
[30] McDonald, C. P., Bachison, C. C., Chang, V., Bartol, S. W., and Bey, M. J., 2010, "Three-Dimensional Dynamic *In Vivo* Motion of the Cervical Spine: Assessment of Measurement Accuracy and Preliminary Findings," Spine **10**(6), pp. 497–504.
[31] Anderst, W. J., Baillargeon, E., Donaldson, W. F., III, Lee, J. Y., and Kang, J. D., 2011, "Validation of a Noninvasive Technique to Precisely Measure *In Vivo* Three-Dimensional Cervical Spine Movement," Spine **36**(6), pp. E393–E400.
[32] Tashman, S., and Anderst, W., 2003, "*In Vivo* Measurement of Dynamic Joint Motion Using High Speed Biplane Radiography and CT: Application to Canine ACL Deficiency," J. Biomech. Eng., **125**(2), pp. 238–245.
[33] An, K. N., Morrey, B. F., and Chao, E. Y., 1984, "Carrying Angle of the Human Elbow Joint," J. Orthop. Res., **1**(4), pp. 369–378.
[34] Chao, E. Y., and Morrey, B. F., 1978, "Three-Dimensional Rotation of the Elbow," J. Biomech., **11**(1–2), pp. 57–73.
[35] ASTM, 1996, "Standard Practice for Use of the Terms Precision and Bias in ASTM Test Methods," West Conshohocken, PA.
[36] Amis, A. A. D. D., Unsworth, A., Miller, J. H., and Wright, V., 1977, "An Examination of the Elbow Articulation With Particular Reference to Variation of the Carrying Angle," Eng. Med., **6**, pp. 76–80.
[37] An, K. N. M., and Morrey, B. F., 2000, "Biomechanics of the Elbow," *The Elbow and its Disorders*, B. F. Morrey, ed., WB Saunders, Philadelphia, pp. 43–60.
[38] Boone, D. C., and Azen, S. P., 1979, "Normal Range of Motion of Joints in Male Subjects," J. Bone Joint Surg. Am., **61**(5), pp. 756–759.
[39] Youm, Y. D. R. F., Thambylajah, K., Flatt, A. E., and Sprague, B. L., 1979, "Biomechanical Analysis of Forearm: Pronation-Supination and Elbow Flexion-Extension," J. Biomech., **12**, pp. 245–255.
[40] Paraskevas, G., Papadopoulos, A., Papaziogas, B., Spanidou, S., Argiriadou, H., and Gigis, J., 2004, "Study of the Carrying Angle of the Human Elbow Joint in Full Extension: A Morphometric Analysis," Surg. Radiol. Anat., **26**(1), pp. 19–23.
[41] Yilmaz, E., Karakurt, L., Belhan, O., Bulut, M., Serin, E., and Avci, M., 2005, "Variation of Carrying Angle With Age, Sex, and Special Reference to Side," Orthopedics, **28**(11), pp. 1360–1363.
[42] Zampagni, M. L., Casino, D., Martelli, S., Visani, A., and Marcacci, M., 2008, "A Protocol for Clinical Evaluation of the Carrying Angle of the Elbow by Anatomic Landmarks," J. Shoulder Elbow Surg., **17**(1), pp. 106–112.
[43] Hurbanek, J. G., Anderson, K., Crabtree, S., and Karnes, G. J., 2009, "Biomechanical Comparison of the Docking Technique With and Without Humeral Bioabsorbable Interference Screw Fixation," Am. J. Sports Med., **37**(3), pp. 526–533.
[44] Rijke, A. M., Goitz, H. T., McCue, F. C., Andrews, J. R., and Berr, S. S., 1994, "Stress Radiography of the Medial Elbow Ligaments," Radiology, **191**(1), pp. 213–216.